Somatic mutations activating STAT3 in human inflammatory hepatocellular adenomas

Camilla Pilati,[1,2] Mohamed Amessou,[1,2] Michel P. Bihl,[1,2] Charles Balabaud,[3] Jeanne Tran Van Nhieu,[4] Valérie Paradis,[5] Jean Charles Nault,[1,2] Tina Izard,[6] Paulette Bioulac-Sage,[3,7] Gabrielle Couchy,[1,2] Karine Poussin,[1,2] and Jessica Zucman-Rossi[1,2,8]

[1]Génomique fonctionnelle des tumeurs solides, Institut National de la Santé et de la Recherche Médicale (Inserm), U674, Paris, F-75010, France
[2]Faculté de Médecine, Université Paris Descartes, Paris, F-75005, France
[3]Inserm, U889, Université Victor Segalen Bordeaux 2, IFR66, Bordeaux, F-33076, France
[4]Department of Pathology, Assistance Publique-Hôpitaux de Paris- CHU Mondor, Créteil, France
[5]Department of Pathology, Assistance Publique-Hôpitaux de Paris, Beaujon Hospital, Clichy, F-92110, France
[6]Department of Cancer Biology, The Scripps Research Institute, Scripps Florida, Jupiter, FL 33485
[7]CHU de Bordeaux, Hopital Pellegrin, Service d'Anatomie Pathologique, Bordeaux, F-33076, France
[8]Department of Oncology, HEGP, Assistance Publique-Hôpitaux de Paris, Paris, F-75015 France

Inflammatory hepatocellular adenomas (IHCAs) are benign liver tumors. 60% of these tumors have *IL-6 signal transducer* (*IL6ST*; gp130) mutations that activate interleukin 6 (IL-6) signaling. Here, we report that 12% of IHCA subsets lacking *IL6ST* mutations harbor somatic *signal transducer and activator of transcription 3* (*STAT3*) mutations (6/49). Most of these mutations are amino acid substitutions in the SH2 domain that directs STAT3 dimerization. In contrast to wild-type STAT3, IHCA STAT3 mutants constitutively activated the IL-6 signaling pathway independent of ligand in hepatocellular cells. Indeed, the IHCA STAT3 Y640 mutant homodimerized independent of IL-6 and was hypersensitive to IL-6 stimulation. This was associated with phosphorylation of tyrosine 705, a residue required for IL-6–induced STAT3 activation. Silencing or inhibiting the tyrosine kinases JAK1 or Src, which phosphorylate STAT3, impaired constitutive activity of IHCA STAT3 mutants in hepatocellular cells. Thus, we identified for the first time somatic *STAT3* mutations in human tumors, revealing a new mechanism of recurrent STAT3 activation and underscoring the role of the IL-6–STAT3 pathway in benign hepatocellular tumorigenesis.

CORRESPONDENCE
Jessica Zucman-Rossi:
zucman@cephb.fr

Abbreviations used: CRP, C-reactive protein; *CTNNB1, catenin* (*cadherin-associated protein*), *β1*; EP, empty plasmid; HCA, hepatocellular adenoma; HCC, hepatocellular carcinoma; *HNF1α*, *hepatocyte nuclear factor 1α*; IHCA, inflammatory HCA; *IL6ST, IL-6 signal transducer*; Luc, luciferase; qRT-PCR, quantitative RT-PCR; SH2, Src homology 2; siRNA, small interfering RNA; STAT3, signal transducer and activator of transcription 3; TAD, transactivation domain.

Inflammatory hepatocellular adenomas (IHCA) are benign liver tumors that predominantly develop in women and are frequently associated with obesity and alcohol abuse (Zucman-Rossi et al., 2006; Bioulac-Sage et al., 2007). These tumors are characterized by overexpression of the acute-phase inflammatory response in tumor hepatocytes and highly polymorphous inflammatory infiltrates. We recently showed that 60% of IHCA activate signal transducer and activator of transcription 3 (STAT3) via somatic heterozygous activating mutations in *IL6ST* (*IL-6 signal transducer*) that encodes the gp130 coreceptor and signal transducer of IL-6 family cytokines (Rebouissou et al., 2009).

Inflammatory adenoma is a homogenous disease in which gp130-mutated and nonmutated IHCAs are similar in their expression profiles, particularly in regard to the expression of acute phase inflammatory response target genes (Rebouissou et al., 2009). To identify genetic alterations causing the inflammatory phenotype, defined as an acute-phase inflammatory response with elevated levels of serum amyloid A and C-reactive protein (CRP) observed in nonmutated gp130 IHCA, we used a candidate gene strategy. We focused on *STAT3*, as it encodes a key nuclear transcription factor that induces the acute-phase inflammatory response

The Rockefeller University Press $30.00
J. Exp. Med. Vol. 208 No. 7 1359-1366
www.jem.org/cgi/doi/10.1084/jem.20110283

The Journal of Experimental Medicine

in hepatocytes. Moreover, STAT3 has oncogenic roles in epithelial cell tumorigenesis (Grivennikov et al., 2009, 2010; Yu et al., 2009). STAT proteins are latent transcription factors activated by phosphorylation, typically after the binding of extracellular ligands to cytokine receptors that activate associated JAK kinases via growth factor receptors having intrinsic tyrosine kinase activity (e.g., epidermal growth factor receptor, platelet-derived growth factor receptor, and colony stimulating factor 1 receptor), as well as by nonreceptor tyrosine kinases such as Src family kinases (Levy and Darnell, 2002). STAT3, one of seven STAT family members, is activated by gp130 in response to IL-6 (Zhong et al., 1994; Inoue et al., 1997). STAT3 is persistently phosphorylated in many human cancer cell lines and in epithelial cells and primary tumors, including hepatocellular carcinoma, breast, prostate, and head and neck cancers, and also in several hematological malignancies. *STAT3* mutations have never been described in human tumors, yet we reasoned that alterations activating its function would explain the inflammatory phenotype of IHCA lacking mutations in gp130.

RESULTS AND DISCUSSION

Identification of STAT3 mutations in IHCA

Among 114 screened hepatocellular adenomas, we identified 7 *STAT3* mutations in 6 tumors (Table I and Fig. S1, A and B). All of these adenomas were inflammatory (6 out of 75 IHCA), and no additional somatic mutations were identified in *hepatocyte nuclear factor 1*α (*HNF1A*), *catenin (cadherin-associated protein),* β*1* (*CTNNB1*), or *IL6ST*, genes that are recurrently altered in IHCA and HCA (Bluteau et al., 2002; Zucman-Rossi et al., 2006; Rebouissou et al., 2009). Thus, *STAT3* IHCA mutations are exclusive from all other known genetic alterations in hepatocellular tumors. STAT3-mutated IHCA were associated with obesity (n = 4) and/or alcohol abuse (n = 3), and multiple (≥4) nodules were present in half of these cases. All *STAT3* mutations were somatic, as they were not observed in adjacent nontumor liver tissues that were steatotic in 5/6 cases. All mutations were also monoallelic and led to amino acid substitutions in 5 cases or to in-frame insertions of 1–4 aa in the remaining 2 cases. In one case (#379), we identified 3 nucleotide mutations that led to amino acid substitutions at codons 502 and 658. Sequencing cloned *STAT3* cDNA from this tumor showed that the three different nucleotide mutations were carried by the same allele. We also showed in three different cases (#379, #966, and #1351) that the mutations were harbored by all of the isoforms of STAT3, including splicing of nucleotides 2099–2101 and 2145–2194 (STAT3β) that lead to p.Ser701del and p.Thr716PhefsX8, respectively (Fig. S1 C; Schaefer et al., 1995). Sequencing *STAT3* RT-PCR products in mutated tumors showed that all cases expressed the normal and mutated *STAT3* alleles at comparable levels (Fig. S1, A and B). Thus, the expression of one mutated *STAT3* allele is a rare but recurrent genetic event in IHCA that is selected for during benign hepatocellular tumorigenesis.

Four of the seven identified mutations were located in the domain of STAT3 (residues 585–688) that shares homology with Src homology 2 (SH2) domains (Fig. 1 A). The STAT3 SH2 domain mediates STAT3 dimerization via binding of phosphotyrosine residue Y705 (Shuai et al., 1994; Wen et al., 1995). Moreover, three of these mutations clustered in a hotspot in the SH2 domain at codons 657 and 658. Interestingly, introduction of cysteine at residues 662 and 664 promotes STAT3 dimerization and creates a constitutively active transcription factor (Stat3-C; Bromberg et al., 1999). The fourth mutation, Y640F, was in the PYTK motif conserved in STAT1, STAT2, and STAT3. Interestingly, substitution of the corresponding Y631 to phenylalanine in STAT2 promotes type I IFN signaling (Scarzello et al., 2007; Constantinescu et al., 2008). The three other mutations found in IHCA were distributed throughout the protein: the altered leucine-78, which contributes to dimerization (Chen et al., 2003); glutamate-166, which is part of helix α1 involved in the interaction with gp130 (Zhang et al., 2000a); and aspartate-502, which is located in the α-helical "connector" domain. Remarkably, none of the mutations identified in IHCA were similar to the 150 germline-inactivating *STAT3* heterozygous mutations described in patients with Job's syndrome, which causes hyper-IgE syndrome (Holland et al., 2007; Minegishi et al., 2007).

IHCA mutations activate STAT3 in absence of IL-6

To investigate possible functional consequences of these STAT3 IHCA mutations, we introduced the seven different IHCA mutations into a *STAT3*α (full-length) cDNA and analyzed their effects in Hep3B cells, a hepatocellular carcinoma line that activates the acute inflammatory phase after treatment

Table I. STAT3 somatic mutations identified in inflammatory hepatocellular tumors

Tumors	Nucleotide change	Amino acid change	Mutant ID
CHC341T	T233>G	L78>R	L^{78}
CHC379T	G1504>T	D502>Y	D^{502}
	A1972>T; G1974>T	K658>Y	K^{658}
CHC574T	G496>C	E166>Q	E^{166}
CHC966T	A1919>T	Y640>F	Y^{640}
CHC1021T	T1969_G1980dup	Y657_M660dup	Y^{657}
CHC1351T	C1968>T; 1969_1970insTTT	G656_Y657insF	G^{656}

Codons and mutated nucleotides are numbered according to *STAT3* cDNA open reading frame.

with IL-6 (Coulouarn et al., 2005). The results were also validated in two additional hepatocellular cell lines (HepG2 and Huh7). As previously described (Bromberg et al., 1999), in the absence of IL-6 ligand and serum, overexpression of WT STAT3 (WT) alone was not sufficient to activate a STAT3 reporter (Fig. 1 B) or the downstream acute-phase inflammatory genes (Fig. 1 C). In contrast, the six IHCA mutants and the mouse Stat3-C mutant (Bromberg et al., 1999) activated the STAT3 reporter in the absence of IL-6 and induced targets typical of the acute inflammatory response, including *CRP* and *SOCS3* (Fig. 1, B and C). Moreover, activation of STAT3 was proportional to the amount of the transfected mutant STAT3 (Fig. 1 D). The last IHCA mutant D502Y/K658Y, identified in tumor #379, has two mutations on the same allele. The D502Y mutation did not impart constitutive activity, whereas K658Y activated the inflammatory response. Additionally, the dual mutant (D502Y + K658Y) produced a hyperactive STAT3 mutant compared with K658Y alone (Fig. 1 E). Thus, mutation at D502 alone is not sufficient to activate STAT3, but cooperates with the mutation at K658 present in the SH2 domain.

IHCA STAT3 mutants are constitutively phosphorylated on Tyr705 and translocate to the nucleus

STAT3 activation requires phosphorylation of tyrosine 705, dimerization, and translocation to the nucleus. Accordingly, in *STAT3*-mutated IHCA, immunohistochemical analyses demonstrated marked overexpression of phospho-Tyr705-STAT3 in the nucleus of these tumor hepatocytes (Fig. 2 A). Similarly, in Hep3B-transfected cells, we showed that the STAT3 mutants L78R, E166Q, Y640F, and G656_Y657insF were constitutively phosphorylated on Tyr705 and translocated to the nucleus, whereas overexpressed WT was unphosphorylated and cytoplasmic in the absence of cytokine (Fig. 2, B–D). STAT3 IHCA mutants did not exhibit increased phosphorylation of serine 727, a second residue involved in STAT3 activation (Wen et al., 1995), when compared with IL-6–activated WT (Fig. S2 A). Moreover, in STAT3 Y640 and G656 mutants,

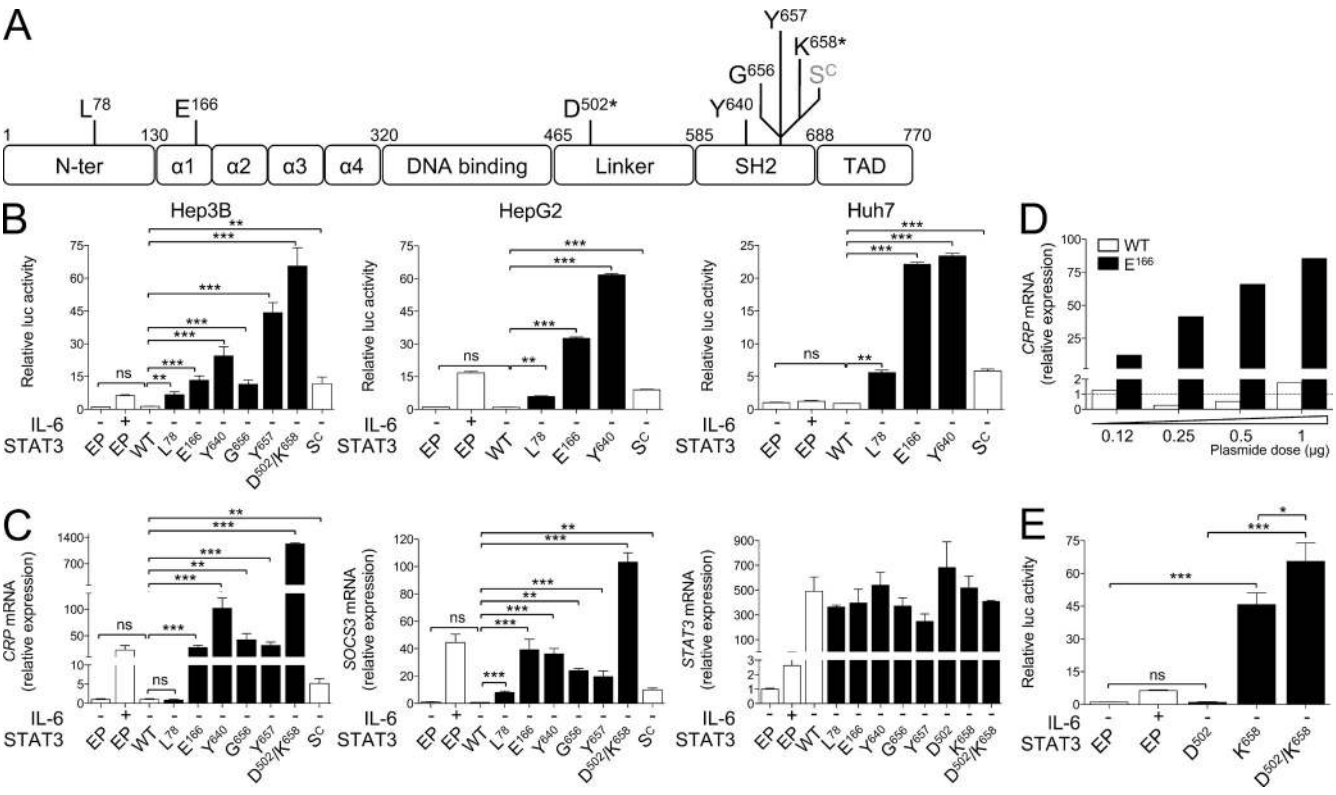

Figure 1. Gain-of-function mutations in STAT3 in IHCA. (A) Distribution of STAT3 mutations identified in IHCA is represented according to the different protein domains. Asterisk indicates the two mutations that are found on the same allele in tumor #379. Stat3-C location is indicated in gray. (B) STAT3 mutants L78R (L^{78}), E166Q (E^{166}), Y640F (Y^{640}), D502Y K658Y (D^{502}/K^{658}), G656_Y657insF (G^{656}), Y657_M660dup (Y^{657}), and Stat3-C (S^C) or control STAT3 WT (WT) and empty plasmid (EP) were transfected in Hep3B, HepG2, and Huh7 cells expressing a STAT3-driven luciferase (Luc) reporter construct. STAT3 activation was measured after 6 h of serum starvation and, when indicated, was treated for 3 h with 100 ng/ml IL-6. Shown is the Luc activity (mean) determined from triplicate co-transfections (± SD) relative to pSIEM-luc alone (EP) without IL-6. (C) Graphs are qRT–PCR results showing the induction of endogenous *CRP*, *STAT3*, and *SOCS3* mRNA after overexpression of mutant STAT3 relative to unstimulated EP-transfected Hep3B cells (EP; mean ± SD). (D) Endogenous *CRP* mRNA expression in Hep3B cells transfected with increasing amounts of expression plasmids encoding WT or E^{166} STAT3 mutant (dotted line: mock-transfected cells). (E) Activity of the STAT3 mutants, including D502Y (D^{502}), K658Y (K^{658}), and the double mutant D502Y K658Y (D^{502}/K^{658}) were evaluated using STAT3-driven Luc in Hep3B cell line. Data are from triplicate transfections (± SD) relative to pSIEM-luc alone (EP). *, $P < 0.05$; **, $P < 0.01$; ***, $P < 0.001$, two-tailed Student's *t* test.

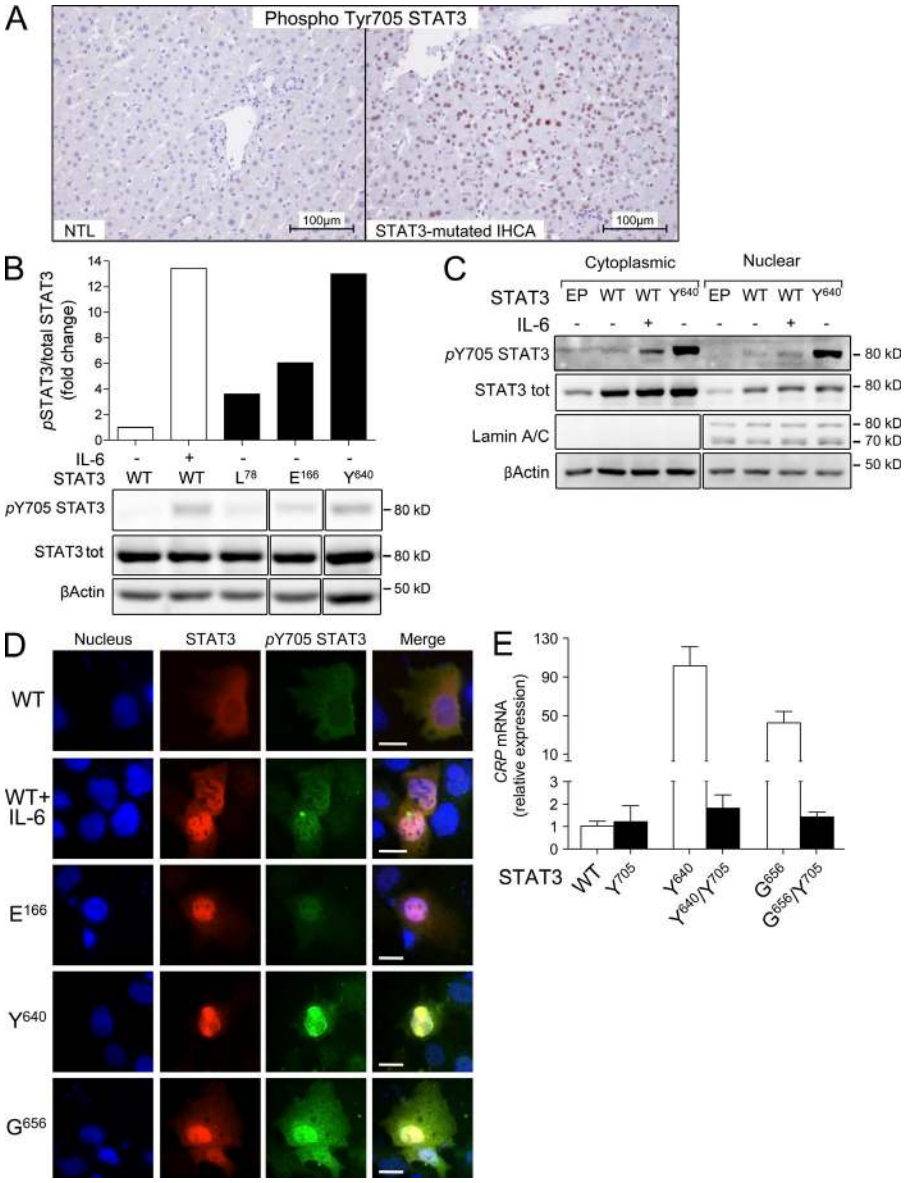

Figure 2. Subcellular localization and role of tyrosine 705 phosphorylation in STAT3 IHCA mutants. (A) Immunochemistry of phospho-STAT3-Y705 in STAT3-mutated IHCA and adjacent nontumor liver (NTL). (B–D) Vectors driving the expression of STAT3 mutants, including L78R (L^{78}), E166Q (E^{166}), Y640F (Y^{640}), G656_Y657insF (G^{656}), or WT (WT) STAT3, were transfected into Hep3B cells. (B) Expression of total and phosphorylated (*p*Y705) STAT3 proteins were assessed by Western blot and bands were quantified with ChemiDoc using the Quantity One software; bars show the expression of *p*Y705 STAT3 relative to total STAT3. (C and D) Subcellular localization of total and phosphorylated (*p*Y705) STAT3 proteins were analyzed by Western blot (C) and by immunofluorescence (D). Results are representative of three independent experiments. Bars, 20 µm. (E) *CRP* mRNA expression after transfection of WT, Y705F (Y^{705}), Y640F (Y^{640}), Y640F/Y705F (Y^{640}/Y^{705}), G656_Y657insF (G^{656}), or G656_Y657insF/Y705F (G^{656}/Y^{705}) STAT3 in unstimulated Hep3B cells. Data are from triplicate transfections (± SD) relative to EP. *, $P < 0.05$; **, $P < 0.01$; ***, $P < 0.001$, two-tailed Student's *t* test.

substitution of tyrosine 705 with phenylalanine totally abrogated activation of the inflammatory response. Thus, tyrosine phosphorylation is essential for activation of IHCA mutant STAT3 (Fig. 2 E).

IHCA STAT3 mutants dimerize in absence of cytokine

A critical step in STAT3 activation is the formation of homodimers through reciprocal phospho-Tyr705–SH2 domain interactions. To assess dimerization by IHCA STAT3 mutants, we performed coimmunoprecipitation assays with epitope-tagged STAT3 proteins. The Y640F mutant homodimerized or heterodimerized with WT independent of IL-6 (Fig. 3 A). Moreover, mutant homodimers were highly phosphorylated at tyrosine 705. In contrast, homodimers of WT were only faintly detected and were not phosphorylated on tyrosine 705. As expected, IL-6 treatment does not enhance dimer formation, but slightly increases tyrosine 705 phosphorylation (Haan et al., 2000). In addition, overexpression of WT impaired the activity of the STAT3 mutant Y640F in a dose-dependent manner (Fig. 3 B). Thus, WT can compete with the mutant STAT3 and impair the formation of active IHCA mutant homodimers. Interestingly, analysis of the STAT3 homodimer structure (Becker et al., 1998) showed that 4 out of 6 STAT3 mutants targeted amino acids (Y640, K658, Y657, and Y657-M660) that reside near the transcription activation domain (TAD; residues 701–722; Fig. 3 C and Fig. S2 B). For example, Tyr-640 engages in hydrophobic interactions with twofold related Phe-710 and residues 656–659 pack against TAD residues 711–716 (Fig. 3 C and Fig. S2 B). These modifications could thus enhance mutant STAT3 function, and they must also somehow facilitate phosphorylation of tyrosine 705 by kinases in hepatocytes, which would then drive dimerization and nuclear localization of mutant STAT3. After cytokine exposure, phosphorylated STAT3 homodimers translocate to the nucleus where they bind to specific IL-6–responsive elements to activate the transcription of target genes (Hattori et al., 1990). In Hep3B cells, nuclear Y640 and G656 STAT3 mutants bind to recognition elements found in endogenous STAT3 target genes in the absence of IL-6, whereas, as expected, WT was defective in binding in the absence of IL-6 (Fig. 3 D).

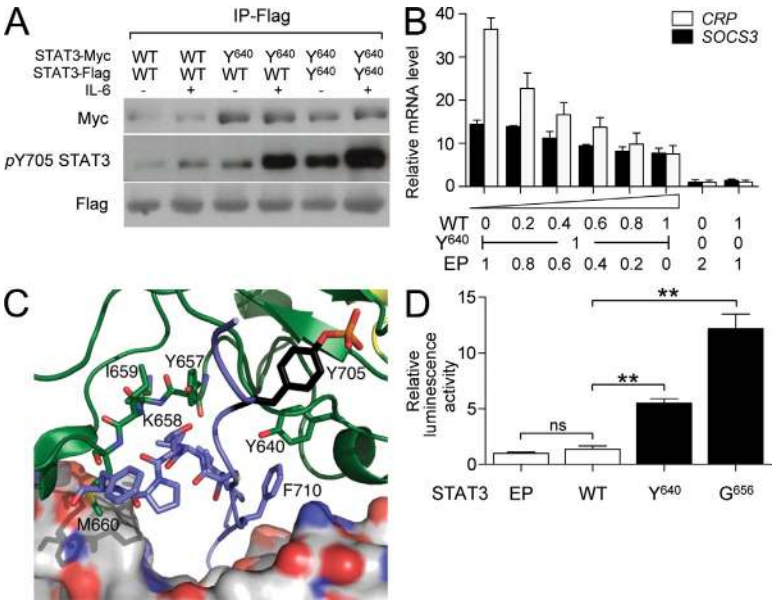

Figure 3. Dimerization of STAT3 IHCA mutants. (A) Flag- and Myc-tagged constructs encoding either WT or mutant Y640 STAT3 were co-transfected (1:1) into Hep3B cells treated, or not treated, with 100 ng/mlIL-6. STAT3 dimer formation was detected after immunoprecipitation using the anti-Flag antibody, followed by immunoblot (IB) analysis with Myc, Flag, and *p*Y705-STAT3–specific antibodies. Results are representative of three independent experiments. (B) Effects of increasing WT STAT3 expression (wedge) on the constitutive activity of Y^{640} mutant STAT3 without IL-6. The graph plots the mean level of expression of *SOCS3* and *CRP* relative to cells transfected with EP (± SD). Units are plasmid micrograms. (C) Several STAT3 IHCA mutations cluster near the TAD of STAT3 (crystal structure; NCBI Protein database accession no. 1BG1; Becker et al., 1998). Residues 640 and 656–660 (shown in green), which are mutated in IHCA tumors, the phosphorylated tyrosine (Tyr-705, black), and TAD residues 711–716 (blue), are shown in stick representation. One polypeptide chain and both TADs are shown as a cartoon. The twofold related molecule, except the TAD, is shown as a surface representation. For residues of the TAD, Tyr-710 of the twofold related molecule is labeled, whereas residues 711–716 are not, for clarity. (D) DNA-binding activity of 10 µg of nuclear extracts of Hep3B cells engineered to express WT, Y^{640}, or G^{656} STAT3 mutants. Bars indicate the DNA-binding activity to consensus STAT3 oligonucleotides relative to activity measured in cells transfected with EP. *, $P < 0.05$; **, $P < 0.01$; ***, $P < 0.001$, two-tailed Student's *t* test. Data are from triplicate transfections (±SD).

IHCA STAT3 mutants are hyperresponsive to IL-6

To investigate the role of the IL-6–JAK pathway in the activation status of IHCA STAT3 mutants, we tested the effects of increasing doses of IL-6 on their activity. Indeed, even low doses of IL-6 (1 ng/ml) dramatically augmented the constitutive activity of the Y640 STAT3 mutant compared with the WT (Fig. 4 A). This hypersensitive response to IL-6 signaling was confirmed for L78, E166, G656, and Y657 STAT3 mutants (Fig. 4 B and Fig. S2 C). Together with gp130, JAK1 is known as the major kinase that phosphorylates and activates STAT3 in IL-6 signaling. Accordingly, silencing JAK1 using small interfering RNA (siRNA) abolished the hyperstimulation of the STAT3 mutants by IL-6 (Fig. 4 B).

Activity of IHCA STAT3 mutants requires Src

In the absence of IL-6 signaling, silencing of gp130 or JAK2 did not affect the constitutive activity of IHCA STAT3 mutants (Fig. 4, C and D). In contrast, JAK1 knockdown by siRNA partially impaired constitutive IHCA STAT3 mutant activity (Fig. 4 E). Similarly, AG490, an inhibitor that disables the kinase activity of both JAK1 and JAK2; Ruxolitinib, a selective inhibitor of Jak1; and curcumin, a STAT3 inhibitor, partially decreased the activity of IHCA STAT3 mutants (Fig. S3, A and B). In contrast, treatment with SrcI-1 kinase inhibitor dramatically impaired both the constitutive and IL-6–induced activation of IHCA STAT3 mutants (Fig. 4 F and Fig. S3 C). Two other Src kinase inhibitors also impaired the activity of IHCA STAT3 mutants (Fig. S3, D and E). Thus, phosphorylation and activation of mutant STAT3 does not require gp130 or JAK2 but requires JAK1 and Src signaling. Depending on cell context, STAT3 can be activated directly by Src family kinases or via Jak1 (in NIH 3T3 cells) as an intermediate kinase between Src and STAT3 (Zhang et al., 2000b). Our findings suggest that in hepatocellular cell lines, the requirement of Jak1 is necessary for maximal activation of IHCA STAT3 mutants, whereas Src is essential for their constitutive activation.

STAT3-mutated IHCA are similar to gp130-mutated IHCA

In vivo, expression analyses of 16 IHCA revealed no significant differences in 28 target genes of IL-6 and IFN signaling pathways in STAT3-mutated adenomas ($n = 5$) versus gp130-mutated IHCA ($n = 11$; Fig. 4 G). Thus, the functional effects of mutating STAT3 and gp130 in human hepatocellular adenomas appear redundant.

In the liver, activation of the IL-6–STAT3 signaling is necessary for the acute-phase response during inflammation (Lütticken et al., 1994) and liver regeneration, particularly after transplantation (Cressman et al., 1996). The connection between inflammation and tumorigenesis has been extensively investigated over the past decade (Grivennikov and Karin, 2010). Depending of the model, inflammation can trigger tumor initiation or function to enhance tumor progression and/or metastasis. During these processes and in numerous tumor types, STAT3 activation has been recognized as a major oncogenic event. However, in our cohort, STAT3-activating mutations were found in 8% of the inflammatory hepatocellular adenoma, but were not present in a series of 218 malignant liver tumors, including hepatocellular carcinomas and cholangiocarcinomas ($n = 11$). Thus, STAT3-activating mutations appear to be largely or quasiexclusively associated with benign proliferation of hepatocytes in human.

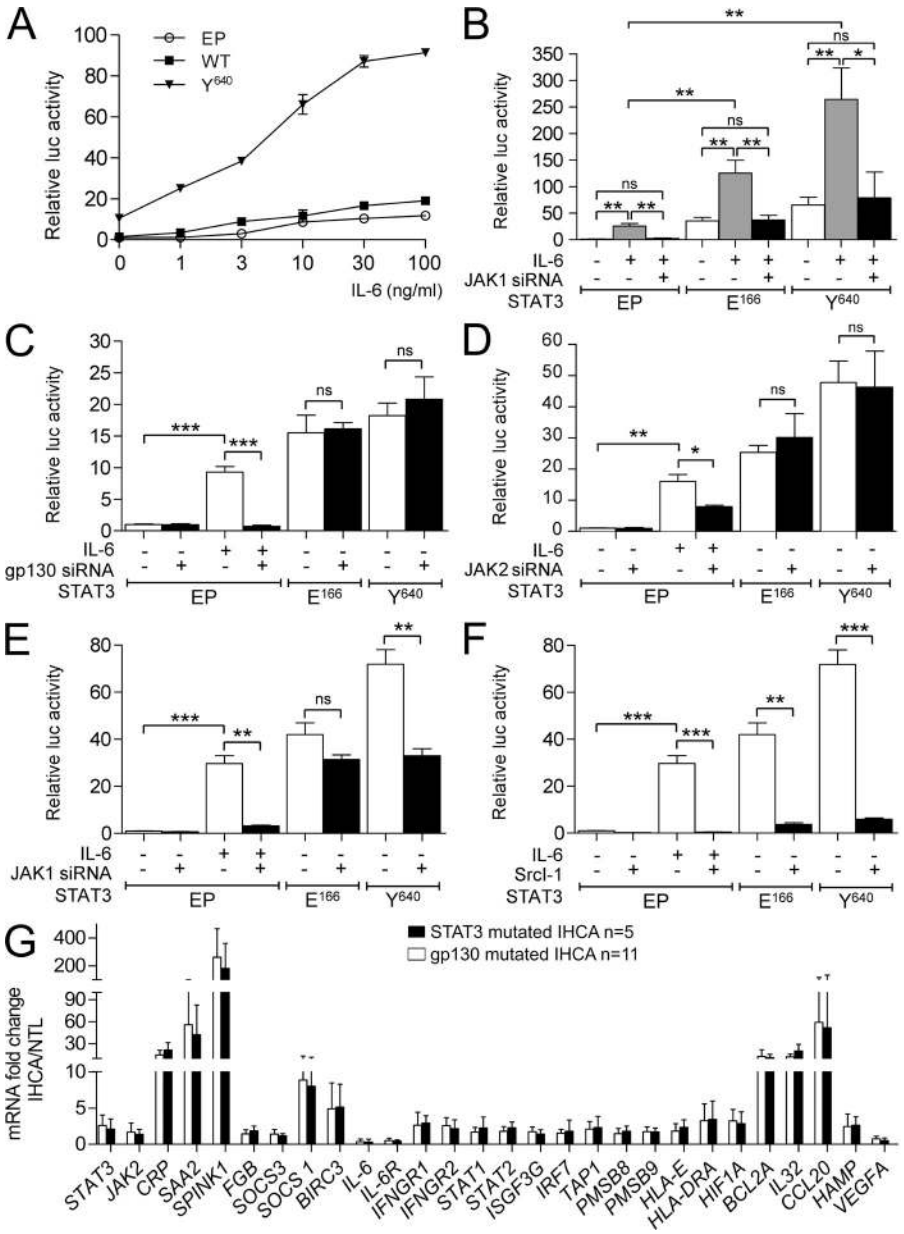

Figure 4. Role of IL-6–JAK pathway and Src kinases on STAT3 IHCA mutant activation. STAT3 mutants Y^{640} and E^{166} were overexpressed in Hep3B cells. Activation of STAT3 is shown by Luc activity (mean) determined from triplicate transfections (± SD) relative to pSIEM-luc alone (EP) with serum starvation. (A) Hep3B cells were exposed to increasing concentrations of IL-6. (B) STAT3 mutants (E^{166} and Y^{640}) or empty vector (EP) were co-transfected with JAK1 siRNA (+) or control siRNA (−) into Hep3B cells exposed to 100 ng/ml IL-6. (C) STAT3 mutants (E^{166} and Y^{640}) or empty vector (EP) were co-transfected with gp130 siRNA (+) or control siRNA (−) into Hep3B cells. (D) STAT3 mutants (E^{166} and Y^{640}) or empty vector (EP) were co-transfected with JAK2 siRNA (+) or control siRNA (−) into Hep3B cells. (E) STAT3 mutants (E^{166} and Y^{640}) or empty vector (EP) were co-transfected with JAK1 siRNA (+) or control siRNA (v) into Hep3B cells. (F) STAT3 mutants (E^{166} and Y^{640}) or empty vector (EP) were transfected into Hep3B cells exposed to Src inhibitor 1 (Srcl-1; 10 μM; 9 h). *, $P < 0.05$; **, $P < 0.01$; ***, $P < 0.001$, two-tailed Student's *t* test. Data are from triplicate transfections (± SD). (G) Expression profiles of STAT3-mutated IHCA and gp130-mutated IHCA. Comparison was performed for the 28 genes validated by qRT-PCR that were significantly differentially expressed between IHCA and nontumorous livers. 5 STAT3-mutated IHCAs (black) were compared with 11 gp130-mutated IHCAs (in white). Results are expressed as mean ± SD; differences between groups are not significant (two-tailed Mann-Whitney test).

Collectively, our findings show that most of the genetic alterations of HCA subtypes (HNF1A inactivation, β-catenin activation, or activation of STAT3 via mutation of STAT3 or gp130), are associated with benign hepatocyte tumorigenesis, where there remains a largely controlled rate of tumor cell proliferation. At present, only β-catenin–activating mutations are associated with malignant transformation to hepatocellular carcinoma (Zucman-Rossi et al., 2006), and here there are likely additional cooperating mutations that lead to frank malignancy. Regardless, to our knowledge this is the first identification of somatic mutation of *STAT3* in human tumors, and these findings underscore the important role of STAT3 activation in hepatocellular benign tumorigenesis and reveal a new mechanism of recurrent STAT3 activation.

MATERIALS AND METHODS

Tumors and patients. A series of 364 hepatocellular tumors, including 114 HCAs, 218 common hepatocellular carcinomas (HCCs), 11 cholangiocarcinomas and 20 hepatocholangiocarcinomas were previously collected (according to French ethical guidelines) and characterized (Bioulac-Sage et al., 2007; Zucman-Rossi et al., 2006). In brief, patients with HCA were predominantly female (80%) with a mean age of 39 yr; among them, 13% presented mutations of *CTNNB1* gene, 19% presented mutations of *HNF1*α, 26% displayed IHCA-associated *IL6ST* mutations, 39.5% showed IHCA without *IL6ST* mutations, and 9.6% were nonclassified adenomas. Patients with HCC were predominantly male (79%), with a mean age of 64 yr, and 34.3% of these presented with cirrhosis. The underlying risk factors of patients with HCC were chronic hepatitis B (19%), chronic hepatitis C (25%) and heavy alcohol intake (38%). Patients with cholangiocarcinoma were predominantly male (72%) and were slightly younger (mean age, 61 yr) than patients with common HCC. Patients with hepatocholangiocarcinoma were also predominantly male (89%) and had a median age of 61 yr. All patients have given consent according to French law, and the ethical committee of Saint Louis Hospital approved the study.

Tumor and nontumor liver samples were frozen immediately after surgery or biopsy and stored at −80°C. Tissues samples were also included in 10% formalin, paraffin-embedded and stained with hematin-eosin and Masson's trichrome. The diagnosis of HCA, HCC, cholangiocarcinoma,

and hepatocholangiocarcinoma was performed using established histological criteria (International Working Party, 1995).

Quantitative RT-PCR (qRT-PCR). qRT-PCR was performed as previously described (Rebouissou et al., 2009) using predesigned primers and probe sets from Applied Biosystems (Table S1). *Ribosomal 18S RNA* (*R18S*) was used to normalize expression data and the 2-ΔΔCT method was applied.

DNA sequencing. DNA sequencing was performed as previously described (Rebouissou et al., 2009) using primers described in Table S2. All HCA samples were previously sequenced for *CTNNB1* (exons 2–4), *HNF1A* (exons 1–10), and *IL6ST* (exon 6). All HCC samples were previously sequenced for *CTNNB1* (exons 2–4) and *P53* (exons 2–10) as previously described (Zucman-Rossi et al., 2006; Rebouissou et al., 2009). All mutations were validated by sequencing a second independent PCR product on both strands. In all cases, the somatic origin of the mutation found in tumor was verified by sequencing the corresponding adjacent, normal liver sample.

Generation of STAT3 mutants. A full-length *STAT3* open reading frame cloned in pCMV6-XL4 vector was purchased from OriGene (SC124165; available from GenBank/EMBL/DDBJ under accession no. NM_139276). Mutagenesis reactions were performed using the QuickChange XL site-directed mutagenesis kit (Stratagene) using primers described in Table S3. All constructs were verified by sequencing. The pCMV6-XL4 expression vector plasmid was used as a control. Stat3-C plasmid was purchased from Addgene, Inc. (plasmid 8722).

Cell culture. Hep3B, Huh7, and HepG2 cells (American Type Culture Collection) were grown in DME containing 10% FCS supplemented with penicillin (100 U/ml) and streptomycin (0.1 mg/ml). For transfections, cells were plated 16 h before transfection to produce monolayers that were 60% confluent, and these were transfected by using either Lipofectamine LTX (plasmid alone) or Lipofectamine 2000 (plasmid and siRNA) according to the manufacturer's instructions (Invitrogen). Transfection efficiency was monitored by measuring the level of WT and mutated *STAT3* mRNA using qRT-PCR or Western blot analysis. The same *STAT3* expression level was observed in WT and IHCA mutant STAT3-transfected cells. For luciferase assays, Hep3B cells were co-transfected with a STAT3 luciferase reporter expressing a firefly luciferase reporter gene that contains three copies of a STAT3 consensus binding site linked to a minimal thymidine kinase promoter (provided by H. Gascan, Institut National de la Santé et de la Recherché Médicale UMR564, Angers, France; pSIEM-Luc 1 µg; Coqueret and Gascan, 2000) and the expression plasmid for WT or IHCA mutant STAT3 (1 µg). 1 d after transfection, cells were starved in a free-serum medium for 3 h, and then left untreated or treated with IL-6 (100 ng/ml) for 3 h. They were then lysed and the luciferase activity was determined according to the manufacturer's recommendations (Promega). The activities were normalized to the protein amounts in each cell lysate. All analyses were performed in triplicate.

Knockdown with siRNA. The efficiency of knockdown using siRNAs was monitored by measuring the level of *JAK1*, *JAK2*, or *IL6ST* mRNA using qRT-PCR (Fig. S3 F) or by Western blot analysis. Knockdown efficiency was >80%. JAK1 siRNA (S7646), JAK2 siRNA (S7651), and IL6ST (gp130) siRNA (S229006) were purchased from Applied Biosystems; siRNA control (Block-IT Alexa Fluor Red) was purchased from Invitrogen.

Pharmacological treatments. Cells were exposed, in serum-free medium, for 6 h to Tyrphostin AG490 (Sigma-Aldrich), 9 h to Src inhibitor-1 (Sigma-Aldrich), Src inhibitor-5 (JS Res Chemical Trading), or PP2 (Sigma-Aldrich); for 18 h to Ruxolitinib (INCB-018424; JS Res Chemical Trading); and for 24 h to Curcumin (Sigma-Aldrich). In the last 3 h of treatment, cells were stimulated with 100 ng/ml IL-6, or not, as indicated.

Western blot analysis. Western blot analyses were performed as previously described (Rebouissou et al., 2009) using antibodies specific for STAT3 (Cell Signaling Technology; 1:500) and phospho-STAT3 Tyr705, (Cell Signaling Technology; 1:200). For dimerization assays, cell lysates were incubated with Immobilized Protein G agarose (Thermo Fisher Scientific) and anti-flag (Cell Signaling Technology; 1:50) or anti-myc (Cell Signaling Technology; 1:200) antibody, at 4°C overnight, before Western blot analysis.

Immunohistochemistry. Immunohistochemistry was performed using a Dako autostainer, on paraffin sections of 10% fixed tumor tissue using a monoclonal anti–phospho-STAT3 Tyr705 (Cell Signaling Technology; 1:50). For each immunohistochemical procedure, antigen retrieval was performed in citrate buffer; detection was amplified by the Dako Envision system.

STAT3 DNA-binding assays. 1 d after transfection, cells were starved in a serum-free medium overnight, and the TransFactor Extraction kit (Takara Bio, Inc.) was used to prepare nuclear extracts following the manufacturer's protocol. Nuclear extracts were analyzed for STAT3 DNA-binding activity using the TransFactor Universal STAT3-specific kits (Takara Bio, Inc.), which is an ELISA-based method.

Immunofluorescence. 24 h after transfection, cells were fixed in 4% formaldehyde for 15 min, washed with PBS, and permeabilized with 0.1% Triton X-100 for 15 min. Cells were saturated with 2% BSA for 30 min, washed with PBS, and then incubated with primary antibody overnight at 4°C. After 3 washes with PBS, cells were incubated with secondary antibodies for 1 h. The slides were washed, and then mounted with VECTASHIELD Mounting Medium with DAPI (Vector Laboratories). Immunofluorescence images were obtained using an HBO 100 optic microscope (Carl Zeiss, Inc.). All data from one experiment were collected at the same intensity and background level. The following monoclonal antibodies were used: rabbit anti–phospho-STAT3 Tyr705 (Cell Signaling Technology; 1:200), mouse anti-total STAT3 (Cell Signaling Technology; 1:100). The secondary antibodies were anti–mouse (Invitrogen; 1:200) and anti–rabbit (Invitrogen; 1:200).

Online supplemental material. Fig. S1 shows the somatic DNA alterations identified on STAT3 gene, and distribution of mutations according to the different isoforms. Fig. S2 shows serine 727 phosphorylation of STAT3 mutants. Fig. S3 shows the effect of inhibitors on STAT3 IHCA mutant activation. Table S1 lists the TaqMan predesigned gene expression assays used for qRT-PCR analyses. Table S2 lists the primers used in PCR and sequencing. Table S2 lists the primers used in in site-directed mutagenesis. Online supplemental material is available at http://www.jem.org/cgi/content/full/jem.20110283/DC1.

We warmly thank Gaelle Cubel for her participation to this work and Hugues Gascan who kindly provided the pSIEM-Luc plasmid. We also thank Jean Saric, Christophe Laurent, Brigitte Le Bail, Anne Rullier, Antonio Sa Cunha for contributing to the tissue collection (CHU Bordeaux) and all the participant to GENTHEP network (Génétique des tumeurs hépatiques).

This work was supported by the association pour la recherche Contre le Cancer (ARC, grant n°3194), Institut National de la Santé et de la Recherche Médicale (Réseaux de recherche clinique et réseaux de recherche en santé des populations), Collection Nationale des Carcinomes Hépatocellulaires, the Ligue Nationale Contre le Cancer ("Cartes d'identité des tumeurs" program) and the BioIntelligence collaborative program. C.P., M.A. and J-C.N. are supported by a fellowship from the MENRT, Inca and ARC, respectively. T.I. is supported by the National Institutes of Health grants GM071596, AI055894, and AI067949.

The authors have no conflicting financial interests

Submitted: 7 February 2011
Accepted: 5 May 2011

REFERENCES

Becker, S., B. Groner, and C.W. Müller. 1998. Three-dimensional structure of the Stat3beta homodimer bound to DNA. *Nature*. 394:145–151. doi:10.1038/28101

Bioulac-Sage, P., S. Rebouissou, C. Thomas, J.F. Blanc, J. Saric, A. Sa Cunha, A. Rullier, G. Cubel, G. Couchy, S. Imbeaud, et al. 2007. Hepatocellular

adenoma subtype classification using molecular markers and immunohistochemistry. *Hepatology*. 46:740–748. doi:10.1002/hep.21743

Bluteau, O., E. Jeannot, P. Bioulac-Sage, J.M. Marqués, J.F. Blanc, H. Bui, J.C. Beaudoin, D. Franco, C. Balabaud, P. Laurent-Puig, and J. Zucman-Rossi. 2002. Bi-allelic inactivation of TCF1 in hepatic adenomas. *Nat. Genet.* 32:312–315. doi:10.1038/ng1001

Bromberg, J.F., M.H. Wrzeszczynska, G. Devgan, Y. Zhao, R.G. Pestell, C. Albanese, and J.E. Darnell Jr. 1999. Stat3 as an oncogene. *Cell*. 98:295–303. doi:10.1016/S0092-8674(00)81959-5

Chen, X., R. Bhandari, U. Vinkemeier, F. Van Den Akker, J.E. Darnell Jr., and J. Kuriyan. 2003. A reinterpretation of the dimerization interface of the N-terminal domains of STATs. *Protein Sci.* 12:361–365. doi:10.1110/ps.0218903

Constantinescu, S.N., M. Girardot, and C. Pecquet. 2008. Mining for JAK-STAT mutations in cancer. *Trends Biochem. Sci.* 33:122–131. doi:10.1016/j.tibs.2007.12.002

Coqueret, O., and H. Gascan. 2000. Functional interaction of STAT3 transcription factor with the cell cycle inhibitor p21WAF1/CIP1/SDI1. *J. Biol. Chem.* 275:18794–18800. doi:10.1074/jbc.M001601200

Coulouarn, C., G. Lefebvre, R. Daveau, F. Letellier, M. Hiron, L. Drouot, M. Daveau, and J.P. Salier. 2005. Genome-wide response of the human Hep3B hepatoma cell to proinflammatory cytokines, from transcription to translation. *Hepatology*. 42:946–955. doi:10.1002/hep.20848

Cressman, D.E., L.E. Greenbaum, R.A. DeAngelis, G. Ciliberto, E.E. Furth, V. Poli, and R. Taub. 1996. Liver failure and defective hepatocyte regeneration in interleukin-6-deficient mice. *Science*. 274:1379–1383. doi:10.1126/science.274.5291.1379

Grivennikov, S.I., and M. Karin. 2010. Inflammation and oncogenesis: a vicious connection. *Curr. Opin. Genet. Dev.* 20:65–71. doi:10.1016/j.gde.2009.11.004

Grivennikov, S., E. Karin, J. Terzic, D. Mucida, G.Y. Yu, S. Vallabhapurapu, J. Scheller, S. Rose-John, H. Cheroutre, L. Eckmann, and M. Karin. 2009. IL-6 and Stat3 are required for survival of intestinal epithelial cells and development of colitis-associated cancer. *Cancer Cell*. 15:103–113. doi:10.1016/j.ccr.2009.01.001

Grivennikov, S.I., F.R. Greten, and M. Karin. 2010. Immunity, inflammation, and cancer. *Cell*. 140:883–899. doi:10.1016/j.cell.2010.01.025

Haan, S., M. Kortylewski, I. Behrmann, W. Müller-Esterl, P.C. Heinrich, and F. Schaper. 2000. Cytoplasmic STAT proteins associate prior to activation. *Biochem. J.* 345:417–421. doi:10.1042/0264-6021:3450417

Hattori, M., L.J. Abraham, W. Northemann, and G.H. Fey. 1990. Acute-phase reaction induces a specific complex between hepatic nuclear proteins and the interleukin 6 response element of the rat alpha 2-macroglobulin gene. *Proc. Natl. Acad. Sci. USA*. 87:2364–2368. doi:10.1073/pnas.87.6.2364

Holland, S.M., F.R. DeLeo, H.Z. Elloumi, A.P. Hsu, G. Uzel, N. Brodsky, A.F. Freeman, A. Demidowich, J. Davis, M.L. Turner, et al. 2007. STAT3 mutations in the hyper-IgE syndrome. *N. Engl. J. Med.* 357:1608–1619. doi:10.1056/NEJMoa073687

Inoue, M., M. Minami, M. Matsumoto, T. Kishimoto, and S. Akira. 1997. The amino acid residues immediately carboxyl-terminal to the tyrosine phosphorylation site contribute to interleukin 6-specific activation of signal transducer and activator of transcription 3. *J. Biol. Chem.* 272:9550–9555. doi:10.1074/jbc.272.14.9550

International Working Party. 1995. Terminology of nodular hepatocellular lesions. *Hepatology*. 22:983–993.

Levy, D.E., and J.E. Darnell Jr. 2002. Stats: transcriptional control and biological impact. *Nat. Rev. Mol. Cell Biol.* 3:651–662. doi:10.1038/nrm909

Lütticken, C., U.M. Wegenka, J. Yuan, J. Buschmann, C. Schindler, A. Ziemiecki, A.G. Harpur, A.F. Wilks, K. Yasukawa, T. Taga, et al. 1994. Association of transcription factor APRF and protein kinase Jak1 with the interleukin-6 signal transducer gp130. *Science*. 263:89–92. doi:10.1126/science.8272872

Minegishi, Y., M. Saito, S. Tsuchiya, I. Tsuge, H. Takada, T. Hara, N. Kawamura, T. Ariga, S. Pasic, O. Stojkovic, et al. 2007. Dominant-negative mutations in the DNA-binding domain of STAT3 cause hyper-IgE syndrome. *Nature*. 448:1058–1062. doi:10.1038/nature06096

Rebouissou, S., M. Amessou, G. Couchy, K. Poussin, S. Imbeaud, C. Pilati, T. Izard, C. Balabaud, P. Bioulac-Sage, and J. Zucman-Rossi. 2009. Frequent in-frame somatic deletions activate gp130 in inflammatory hepatocellular tumours. *Nature*. 457:200–204. doi:10.1038/nature07475

Scarzello, A.J., A.L. Romero-Weaver, S.G. Maher, T.D. Veenstra, M. Zhou, A. Qin, R.P. Donnelly, F. Sheikh, and A.M. Gamero. 2007. A Mutation in the SH2 domain of STAT2 prolongs tyrosine phosphorylation of STAT1 and promotes type I IFN-induced apoptosis. *Mol. Biol. Cell*. 18:2455–2462. doi:10.1091/mbc.E06-09-0843

Schaefer, T.S., L.K. Sanders, and D. Nathans. 1995. Cooperative transcriptional activity of Jun and Stat3 beta, a short form of Stat3. *Proc. Natl. Acad. Sci. USA*. 92:9097–9101. doi:10.1073/pnas.92.20.9097

Shuai, K., C.M. Horvath, L.H. Huang, S.A. Qureshi, D. Cowburn, and J.E. Darnell Jr. 1994. Interferon activation of the transcription factor Stat91 involves dimerization through SH2-phosphotyrosyl peptide interactions. *Cell*. 76:821–828. doi:10.1016/0092-8674(94)90357-3

Wen, Z., Z. Zhong, and J.E. Darnell Jr. 1995. Maximal activation of transcription by Stat1 and Stat3 requires both tyrosine and serine phosphorylation. *Cell*. 82:241–250. doi:10.1016/0092-8674(95)90311-9

Yu, H., D. Pardoll, and R. Jove. 2009. STATs in cancer inflammation and immunity: a leading role for STAT3. *Nat. Rev. Cancer*. 9:798–809. doi:10.1038/nrc2734

Zhang, T., W.H. Kee, K.T. Seow, W. Fung, and X. Cao. 2000a. The coiled-coil domain of Stat3 is essential for its SH2 domain-mediated receptor binding and subsequent activation induced by epidermal growth factor and interleukin-6. *Mol. Cell. Biol.* 20:7132–7139. doi:10.1128/MCB.20.19.7132-7139.2000

Zhang, Y., J. Turkson, C. Carter-Su, T. Smithgall, A. Levitzki, A. Kraker, J.J. Krolewski, P. Medveczky, and R. Jove. 2000b. Activation of Stat3 in v-Src-transformed fibroblasts requires cooperation of Jak1 kinase activity. *J. Biol. Chem.* 275:24935–24944. doi:10.1074/jbc.M002383200

Zhong, Z., Z. Wen, and J.E. Darnell Jr. 1994. Stat3: a STAT family member activated by tyrosine phosphorylation in response to epidermal growth factor and interleukin-6. *Science*. 264:95–98. doi:10.1126/science.8140422

Zucman-Rossi, J., E. Jeannot, J.T. Nhieu, J.Y. Scoazec, C. Guettier, S. Rebouissou, Y. Bacq, E. Leteurtre, V. Paradis, S. Michalak, et al. 2006. Genotype-phenotype correlation in hepatocellular adenoma: new classification and relationship with HCC. *Hepatology*. 43:515–524. doi:10.1002/hep.21068